CONCRETE LIBRARY OF JSCE. NO. 21, JUNE 1993

DETECTION OF FINE CRACKS IN REINFORCED CONCRETE THROUGH X-RAY TECHNIQUES USING CONTRAST MEDIA

(Reprint from Transaction of JSCE, Vol. 17, No. 451, 1992)

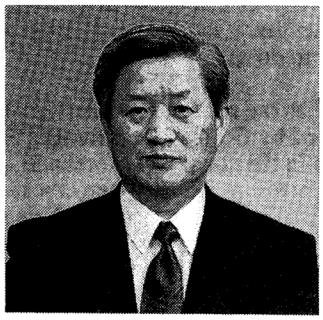

Koji OTSUKA

SYNOPSIS

Experiments were carried out to develop a new nondestructive x-ray inspection technique for concrete using contrast media. Satisfactory results were obtained. A contrast medium suitable for the investigation was selected by comparisons of the numerous varieties used in the medical field. Employing the new technique, patterns of fine cracks were detected in concrete around deformed bars of axially loaded tensile specimens, lapped splice specimens, and beam specimens. The crack patterns on the x-ray plates were compared with those obtained by the red ink injection method. Three-dimensional images of cracks in concrete and the influence of aggregate size on cracking pattern were also examined.

Keywords: non-destructive test, x-ray inspection technique, contrast medium, internal fine crack

---

K. Otsuka is a professor of civil engineering at Tohoku Gakuin University, Tagajo, Japan. He received his Dr. Eng. degree from Tohoku University in 1981. His research interests are the bonding and cracking of reinforced concrete. He holds membership of JSCE, JCI, CEB, ACI, and IABSE.

1. INTRODUCTION

Reinforced concrete is a multiple composite structure of concrete, itself a composite material, bonded to reinforcing steel. Its mechanical behavior changes in an extremely complex manner according to conditions of loading and environment. Of particular effect on its behavior are the cracks that occur in the concrete. These cracks are not only those visible at the surface; numerous minute cracks from within the concrete also and their occurrence, accumulation, connections and growth are the causes of concrete's nonlinear behavior. Characteristics such as the orientation and number of internal cracks formed in concrete around deformed bars bear a close relationship to the force transmission mechanism between reinforcement and concrete. Accordingly, to express rationally the mechanical behavior of reinforced concrete in a way that takes into consideration the mechanism by which this occurs, it is necessary to know the properties of these minute cracks inside the concrete.

Observation of fine cracks on the concrete's surface can be done by various means, such as optical microscope, electron microscope, holographic moire, laser spectrum, etc. However, there are cases when the stress conditions differ between the surface of the concrete and its interior; in particular, the minute cracks that occur in concrete around deformed bars cannot be observed at the surface. Consequently, it is necessary to observe the cracks actually inside the concrete, but there are few ways to do so.

The author, in the past, has used as the method of observing internal cracks known as the "red ink injection method" as developed by Goto and the author [1], [2]; in this technique, red ink is injected into small holes formed in the concrete beforehand, and the ink enters internal cracks taking advantage of the negative pressure arising when cracks are formed. Later, the concrete is split longitudinally to reveal the interior for inspection. This method has the merit of allowing internal cracks to be directly observed by eye, but there the drawback is that the condition under which cracking occurs and growth of the cracks with increasing reinforcing bar stress cannot be observed using a single specimen.

X-ray inspections have been employed in the past as a method of nondestructively examining cracks and internal defects in concrete. However, it is not possible to detect fine cracks inside concrete using ordinary x-ray techniques.

It was thought by the author that, by injecting a contrast medium into small holes made in the concrete in place of red ink and then performing radiography the occurrence and growth of fine cracks might be continuously detected. To this end, basic experiments were conducted to develop this technique. The properties of the fine cracks detected by this x-ray technique were compared with the results of the red ink injection method, while the three-dimensional configurations of internal cracks and the influence of maximum coarse aggregate size were also studied.

2. MATERIALS USED IN TESTS AND TESTING METHOD

2.1 Specimens and Loading Method

Mortar and concrete containing high-early- strength portland cement were used in the tests. Both coarse and fine aggregates were river products with maximum sizes of 5 mm (mortar) and 10 and 15 mm (concrete). The mixes all had water-cement ratios of 0.5, while the ratio by weight of fine and coarse aggregate was made 1:1.

Specimens were of the three kinds of reinforced concrete: axially tensioned specimens (using D16 reinforcing bars); lapped splice specimens (using D16 reinforcing bars); and beam specimens (using D6 reinforcing bars). Their shape and dimensions were as shown in Fig. 1. Specimens of comparatively small size were used due to the range of the x-ray apparatus and the

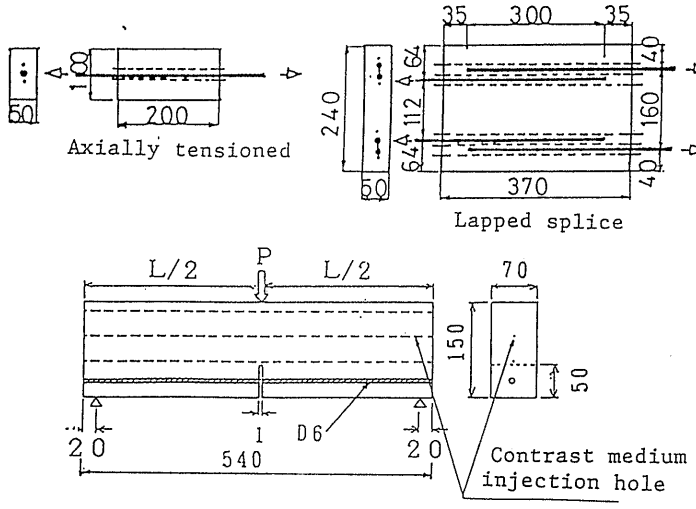

Fig. 1 Configurations and dimensions of specimens

size of the film. The thicknesses of specimens were set at 50 and 70 mm in view of the results of preliminary tests on x-ray penetration effects. Several small-diameter holes (I.D. 2 mm) parallel to the reinforcing bars were formed in the specimen concrete beforehand to allow injection of the contrast medium.

A universal testing machine was used for loading in the cases of axially tensioned and lapped splice specimens. The load was increased in stages (of 250 kgf/cm^2 (24.5 MPa) in reinforcement tensile stress intensity in the case of axially tensioned specimens, and 125 kgf/cm^2 (12.3 MPa) in the case of lapped splice specimens), and contrast medium radiography was performed at each stage. Axially tensioned specimens were loaded while under a lateral pressure of 30 kgf/cm^2 (2.9 MPa) provided by a load cell in a longitudinal direction on a surface perpendicular to the reinforcing bar axis.

In the case of beam specimens, center point loading was carried out by attaching a device for flexural testing to the universal testing machine. The load was gradually increased and loads were measured with a load cell. Crack opening displacement was measured using a displacement meter straddling a notch in the meddle of the span in the tension zone. These instruments were monitored by an X-Y recorder, and contrast medium radiography was performed at several stages around the maximum load and in the strain-softening range.

2.2 Contrast Medium

Contrast media, generally find widespread use in the field of medicine; they are substances that cause a difference in the penetration rates of x-rays between organs inspected and surrounding tissue. Contrast media are either positive media, which have x-ray absorption rates higher than the surrounding tissue, meaning they appear as white shadows on exposed film, and negative contrast media with x-ray absorption rates lower than the surrounding tissue and showing up as black on exposed film. There are great variations in the composition, concentration, and viscosity of the contrast media in use. Consequently, there was a need to select a medium suiting the objectives of this study. The following conditions were taken into consideration in making the selection:

Table 1 Commercial contrast media used in performance comparison tests

Symbol	Active component	Total salt concentration w/v%
A	Barium sulfate	140.0
B	Barium sulfate	75.0
C	Barium sulfate	100.0
D	Barium sulfate	120.0
E	Organic iodine compound	60.0
F	Organic iodine compound	30.0
G	Organic iodine compound	82.3

Note) A consisted of 300 g of powder suspended in 135 cc of water

(1) That an adequate difference in x-ray absorption rates is produced between cracked portions and the surrounding concrete and that sharp images of cracks are obtained.

(2) That injection into fine cracks is possible.

(3) That the substance is chemically stable, nontoxic, and safe to handle.

(4) That it is comparatively inexpensive.

Of these conditions, tests need to be performed to ensure compliance with (1) and (2), but four varieties of barium sulfate based media and three varieties of organic iodine based media were selected based on their composition and concentration, and because they comply with (3) and (4). They are listed in table 1. Each medium was subjected to comparative experiments on x-ray imaging effects and crack penetration properties.

Tests to compare the performances of contrast media were firstly image extinguishing voltage and kinematic viscosity measurements. Next, radiography was carried out on concrete specimens for a performance comparison and experiments to confirm performances were also conducted.

If it were possible to check all the varieties and mixes of their constituents, the radiographic performance of media could be readily compared by computing mass absorption coefficients. However, various chemicals are added to the contrast media used for medical purposes to prevent side effects on the human body, and the exact ingredients and composition are often not clearly indicated. The method of measuring the image extinguishing voltage was devised to enable performance comparisons of commercial contrast media for which the constituents are not published. In these measurements, a contrast medium in liquid form is injected into a plastic pipe (I.D. 3 mm), the pipe is irradiated with x-rays, and when observations are carried out in TV mode, the contrast medium absorbs x-rays, so the pipe appears as a straight black line. As the x-ray tube voltage is gradually increased, the black line gradually becomes lighter in color and eventually disappears. The voltage at that time we call the image extinguishing voltage. Performance was compared taking advantage of the property that the image extinguishing voltage is proportional to the imaging performance.

Kinematic viscosity measurements were made for the purpose of comparing the ability of liquid contrast media to penetrate into cracks. The internal friction produced when a fluid moves is called viscosity and viscosity (μ) divided by the density (ρ) of the fluid is called the kinematic viscosity ($\nu = \mu/\rho$).Measurements were made using a Cannon-Fenske viscometer.

Experiments to ascertain the injection ability and contrast performances of the individual contrast

media relative to cracks actually formed in concrete were conducted by embedding single D16 reinforcing bars for axial tensioning along the central axes of specimens. The specimens were 50 x 100 mm in cross section and with lengths of 200 mm. Each had two injection holes of diameter approximately 2 mm slightly separated from and parallel to the reinforcing bars. Contrast media was injected into these holes and radiography was carried out.

2.3 X-ray Inspection Technique and Crack Detection Systems

X-ray inspections consisted of pumping a contrast medium into the injection holes in specimens prior to loading, and performing radiography continuously or at certain stages during loading. The systems used for detecting cracks, of which shadowgraphs were taken, as shown in Fig. 2, were two kinds of "film mode" directly onto x-ray film and the "TV mode" using a x-ray image amplifier.

In the film mode, the distance between the specimen and x-ray generating apparatus was fixed at 60 cm, film was placed in close contact with the specimen, and irradiation was carried out for 3 minutes at tube voltages of 100 to 120 kV and current of 2 mA. Films used were #100 industrial x-ray film. The film mode has the advantage that if the dimension of the film are matched to the dimensions of the specimen, the condition of cracking over the entire specimen can be detected simultaneously, the resolution is good, and extremely fine cracks can be detected if a Scharkasten (film viewing device) is used. However, there are drawbacks; irradiation for about 3 minutes is required for filming and it is necessary to maintain a constant load during that time. This means that load cannot be increased continuously during testing.

In the TV mode, the distance between the x-ray generating apparatus and the specimen was fixed at about 90 cm and the distance between the specimen and image amplifier about 25 cm. A tube voltage of 50 to 60 kV and a current of 2 mA was used. While observing the TV monitor images in real time during loading, a VTR recording was also made, and interesting areas were later subjected to a high degree of picture processing to obtain hard copies. The TV mode has the advantage that cracks can be detected in real time and that, if a VTR is used, rapid failure can be later resolved into single frames. The drawbacks are that picture quality is rather poor compared with the film mode even when sophisticated picture processing is done, and the range of image size (a circle of diameter 180 mm) is limited.

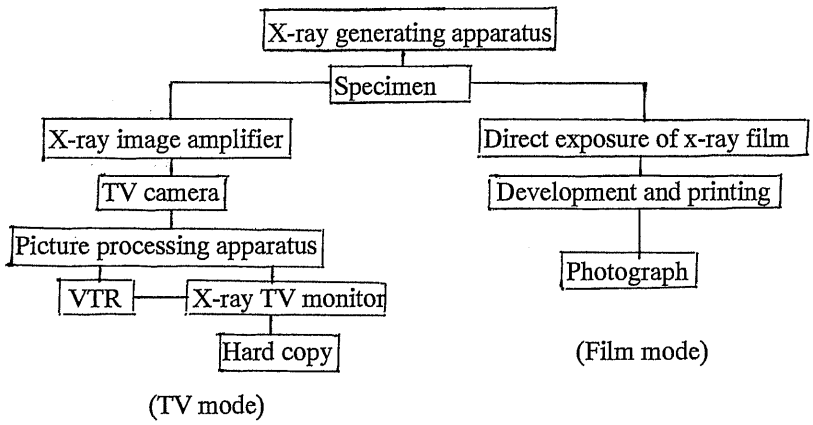

Fig. 2 Crack detection system

3. RESULTS OF CONTRAST MEDIA PERFORMANCE COMPARISON TESTS

3.1 Image Extinguishing Voltage

The results of measurements of image extinguishing voltage are given in Table 2. As this table shows, the voltages were highest with the barium sulfate contrast media A and D, followed by barium sulfate base C, and organic iodine base G. The lack of great difference in these image

Table 2 Results of contrast media performance comparison tests

Symbol	Component	Image extinguishing voltage ekv	Kinetic viscosity cm^2/s
A	Barium sulfate	43.0	10.5
B	Barium sulfate	41.0	72.7
C	Barium sulfate	42.0	69.2
D	Barium sulfate	43.0	19.5
E	Organic iodine compound	38.5	5.4
F	Organic iodine compound	37.5	2.1
G	Organic iodine compound	42.0	12.8

Note) A consisted of 300 g of powder suspended in 135 cc of water.

extinguishing voltages is because comparisons were made of contrast media in practical use in the medical field. However, since these values correlate with the total salt concentration in the respective component, it is thought they can be used for comparisons of their image producing performance.

3.2 Kinematic Viscosity

The results of kinematic viscosity measurements are given in the right-hand column of Table 2. As this table shows, barium sulfate based media are generally of great kinematic viscosity, A being an exception. The medium with the least viscosity is F, while G has the greatest viscosity among the organic iodine based media, but it is still quite low compared with B, C, and D.

3.3 Ascertainment of Performance in Concrete

Various contrast media were actually injected into specimens to compare their performance in concrete; the following is a description of the results of injection and image tests. Four of the barium sulfate contrast media could be readily injected into comparatively large injection holes, and the shadows of these holes were distinctly seen in the radiographs. However, hardly any of the fine internal cracks occurring around the deformed bars was registered. This, as can be comprehended from the kinematic viscosity measurements given in 3.2, is likely to have been because barium sulfate based contrast media are highly viscous in general, and it was not possible for injection to be achieved into fine cracks (normally 0.01 mm wide and under) under the action of the negative pressure set up when internal cracks are formed. Contrast medium A was of relatively low kinematic viscosity, but this was a material consisting of powder suspended in water and easily segregated, and it is thought that only water entered the fine cracks. The three kinds of organic iodine based contrast media, when the manner in which the large injection holes appear is compared, are slightly inferior to barium sulfate based media, but it was possible for them to enter the fine internal cracks, and this was confirmed by radiography. It was ascertained that contrast medium G, with the highest content of iodine (440 mg/ml), offered the best image performance of the three varieties of iodine based media. Based on these experimental results, it was confirmed that contrast medium G, although slightly high in viscosity, was capable of being injected into fine cracks and, moreover, offered the greatest contrast; therefore, it was used for subsequent tests as the medium most suited to the objectives of this study

4. RESULTS OF EXPERIMENTS FOR DETECTION OF FINE CRACKS

4.1 Axially Tensioned Specimens

Photograph 1 gives as an example of the results obtained in detecting fine cracks by radiography; this is a case of an axially tensioned specimen (with a concrete cross section of 50 x 100 mm, a length of 200 mm, and with a single D16 reinforcing bar on the central axis). It is part of a x-ray shadowgraph at a reinforcing bar stress of 3,720 kg/cm^2 (365 MPa). Numerous fine cracks in a complex configuration in the vicinity of the lugs on the deformed bar are detected. Near the ends, the separation of the reinforcing bar and concrete can be clearly seen. On directly observing the x-ray film after radiography using a Scharkasten, even extremely fine cracks can be discerned as differences in the shading of the shadows, however, when printed on photographic paper, it tends to become more difficult to distinguish fine cracks. The cracks seen through the Scharkasten in the case of Photo 1 were directly traced and are shown in Fig. 3. As can be seen, there are many fine cracks extending outwards from the lugs of the deformed bars in the concrete.

In Fig. 4, images of fine crack occurrence at five stages - from the time of first detection - for a different specimen under the same conditions as in Photo 1 are shown. These figures show that internal cracks are formed first at the lugs on the reinforcing bar near the end of the specimen, next near the middle of the specimen, and then, as the stress intensity in the reinforcing bars increases, the number and extent of cracks gradually increase. Further, whereas the direction of growth of cracks formed near the end of a specimen is towards the end, cracks formed in the middle of the specimen grow in a direction perpendicular to the reinforcing bar axis, becoming interwined in a complex pattern. The number and range increase, and finally, the cracks reach the extremities of the specimen.

Examples of the red ink injection method are shown in Photo 2 for axially loaded tensile specimens for a comparison of the radiography and red ink injection methods. It is clear that the location and general configuration of cracking, such as its inclination, is similar to that obtained by the red ink injection method, but there are also significant differences. The principal points of difference are as follows.

(1) Using the x-ray contrast medium technique, the presence of fine cracks in the concrete was detected for the first time at a reinforcing bar stress intensity of around 1,500 kgf/cm^2 (147 MPa); with the red ink injection method, however, cracks were detected even below about 1,000 kgf/cm^2 (98 MPa).

(2) According to the x-ray technique, there were same lugs at which no cracks were detected, but with the red ink injection method cracks were at just about all lugs.

(3) In radiography, many fine cracks of complex configuration were detected at individual lugs, but with the red ink injection method, a single crack of comparatively simple configuration was detected at each lug in almost all cases.

Of these differences, the following is thought to account for (1) and (2). When transmitting x-ray through the interior of the concrete and registering an image, even it a contrast medium is used, there may be limits to fine-crack detecting capabilities compared with the red ink injection method, in which the concrete is actually split and the interior observed. As for the reasons for point (3) above, the following may be considered a suitable explanation. In radiography, cracks across the thickness of the concrete specimen are summed, and the film may register all of them. Consequently, even a single crack, if it has a complex three-dimensional configuration, would probably be detected on film as a multitude of cracks. An experimental study was carried out regarding this possibility for (3) and the results are described in 4.4.

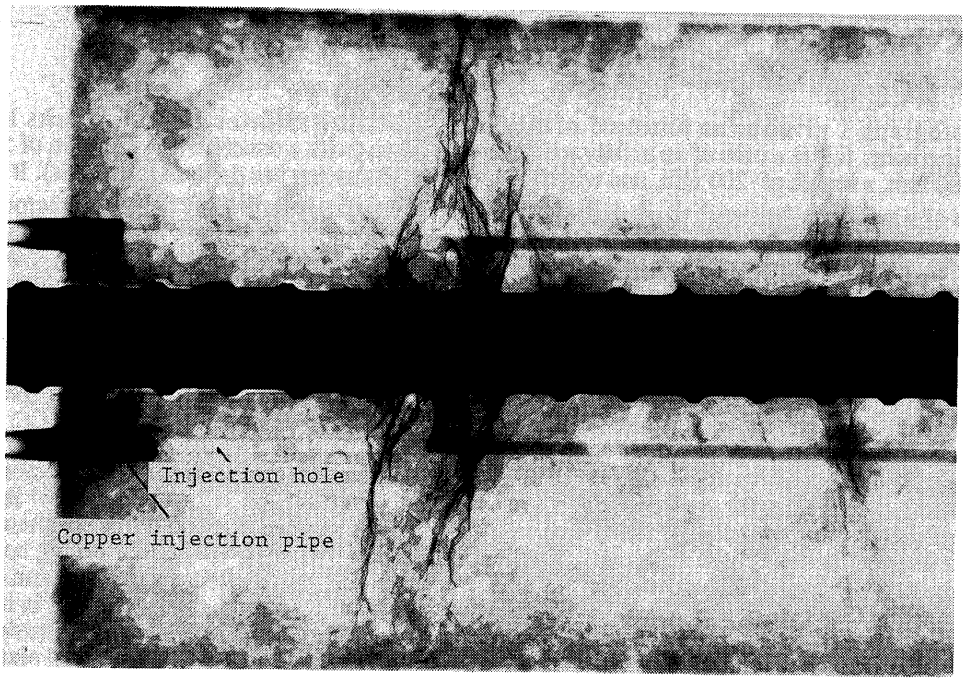

Photo. 1 Results of fine cracks detection by the x-ray technique: axially tensioned specimen [6] (reinforcing bar: D16; reinforcing bar stress: 3,720 kgf/cm^2 (365 MPa); maximum size of aggregate 10 mm)

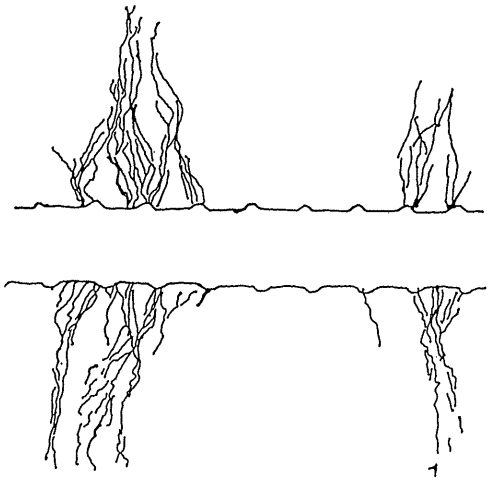

Fig. 3 Diagram traced from x-ray film (Photo. 1) [6]

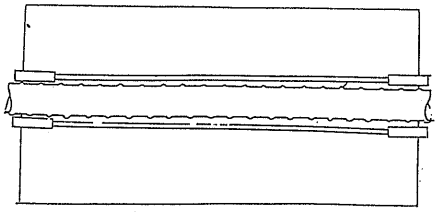

a. Condition of cracking at reinforcing bar stress: 1,570 kgf/cm^2 (154 MPa)

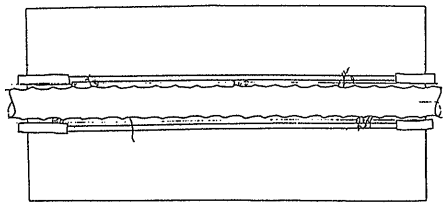

b. Condition of cracking at reinforcing bar stress: 2,620 kgf/cm^2 (257 MPa)

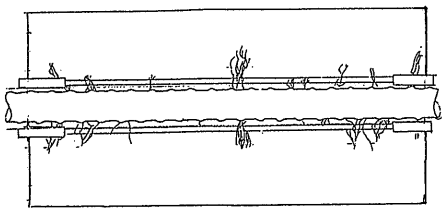

c. Condition of cracking at reinforcing bar stress: 3,140 kgf/cm^2 (308 MPa)

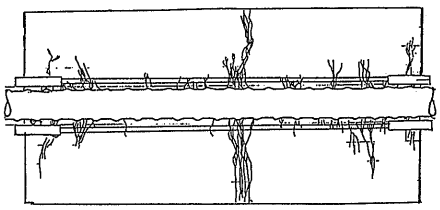

d. Condition of cracking at reinforcing bar stress: 3,660 kgf/cm^2 (359 MPa)

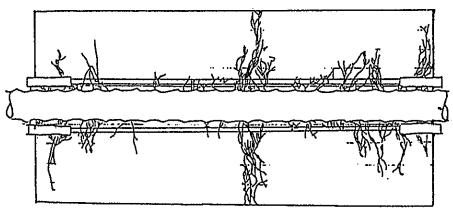

e. Condition of cracking at reinforcing bar stress: 3,730 kgf/cm^2 (366 MPa)

Fig. 4 Crack growth in axially tensioned specimen (traced from x-ray shadowgraph film, reinforcing bar: D16; maximum size of aggregate: 15 mm)

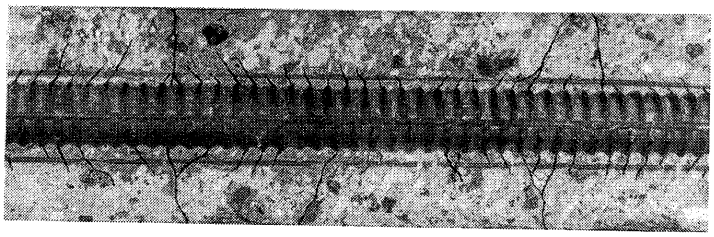

Photo. 2 Internal cracks occurrence obtained by ink injection method (reinforcing bar: D51; reinforcing bar stress: 3,000 kgf/cm^2 (294 MPa); maximum size of aggregate: 25 mm

4.2 Lapped Splice Specimen

Photograph 3 is a shadowgraph at a reinforcing bar stress intensity of 2,400 kgf/cm^2 (235 MPa) as an example of the results of fine crack detection by radiography on a lapped splice specimen (concrete cross section 50 x 240 mm, length 370 mm, D16 reinforcing bars placed with clear spacing of approximately 8 mm and lapped length of 30 cm, two sets of these lapped splices arranged in parallel). As the photograph shows, numerous internal cracks formed, linking the two lapped reinforcing bars. The angle of these internal cracks to the reinforcing bar axis is scattered between 30 and 40 deg, and multiple fine cracks can be detected occurring from a single lug.

Further, at the ends of the splice, lateral cracks (primary lateral cracks) were seen perpendicular to the reinforcing bar axis at the specimen surface while the load was comparatively low, but this did not show up distinctly on the film. This is thought to have been because, when injecting the contrast medium as shown in the photograph, the copper injection tubes were inserted somewhat beyond the end of the splice to ensure adequate adhesion in the concrete. As a result, the contrast medium failed to be injected into the primary lateral cracks at the end of the splice.

Figure 5 shows the fine crack formation as directly traced from x-ray films in four stages beginning at the time cracks were first detected and ending at the reinforcing bar stress immediately before joint failure. It can be seen that as the tensile stress on the reinforcing bars increases, a number of fine internal cracks - later to become the source of primary lateral cracks - firsts occur perpendicularly to the reinforcing bar axis. These grow until they reach the surface of the specimen. Next, fine cracks begin to occur diagonally from locations on the surfaces of the reinforcing bars near these original cracks and the number of these cracks gradually increases.

For comparison, Photograph 4 shows the occurrence of internal cracks in the case of a lapped splice specimen obtained by the red ink injection method. Comparing the fine cracks in Photo. 3 and Fig. 5 with Photo. 4, it may be concluded that the locations of cracks and their angles are in general similar. However, regarding the number of cracks occurring from a single lug, more are visible in Photo. 3 and Fig. 5, and considerable more in the area between the two lapped reinforcing bars.

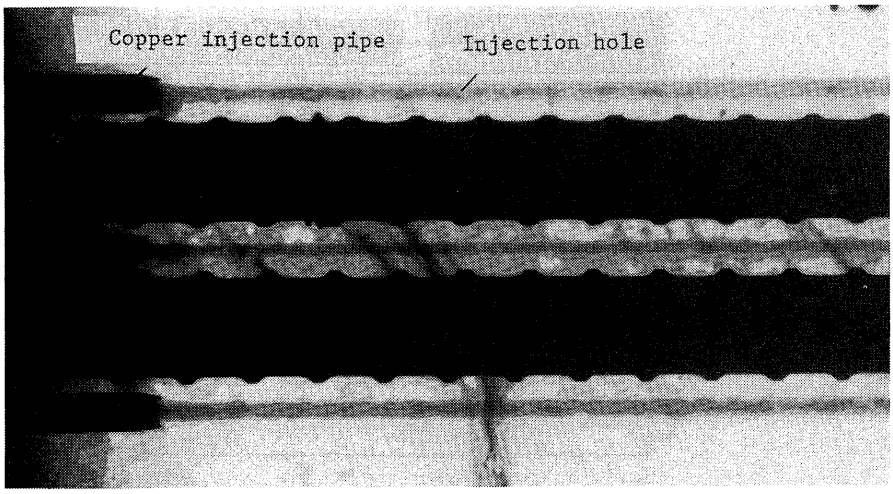

Photo. 3 Results of fine crack detection by the x-ray technique: lapped splice specimen (reinforcing bar: D16; reinforcing bar stress: 2,400 kgf/cm^2 (235 MPa); maximum size of aggregate: 5 mm)

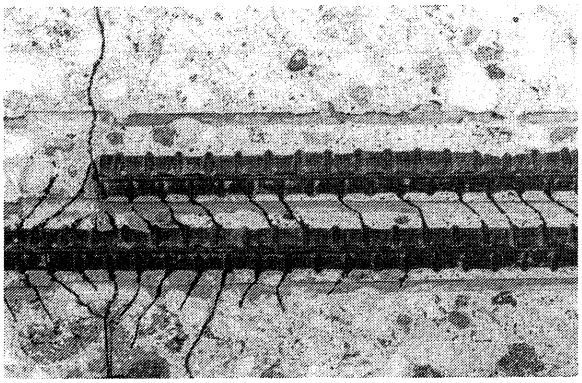

Photo. 4 Crack occurrence obtained by ink injection method (reinforcing bar: D16; lapped length: 25 cm; reinforcing bar stress: 2,500 kgf/cm^2 (245 MPa); maximum size of aggregate: 25 mm)

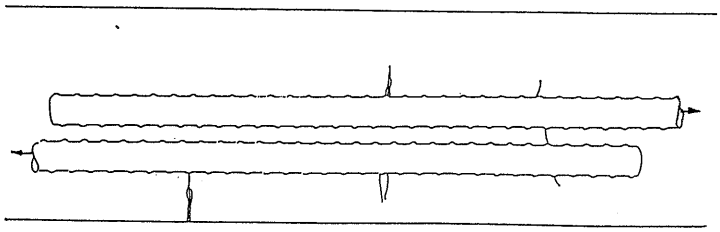

a. Reinforcing bar stress: 1,350 kgf/cm^2 (132 MPa)

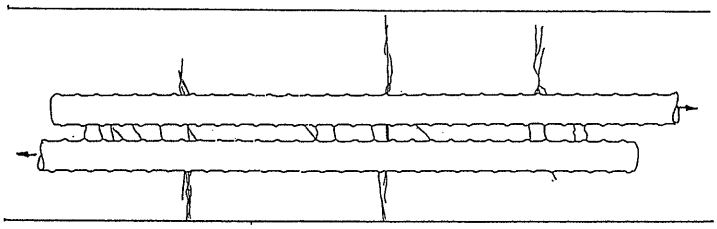

b. Reinforcing bar stress: 1,600 kgf/cm^2 (157 MPa)

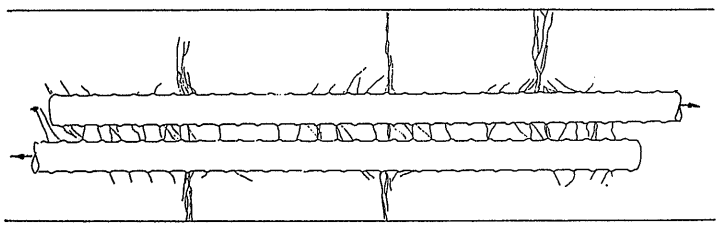

c. Reinforcing bar stress: 1,770 kgf/cm^2 (173 MPa)

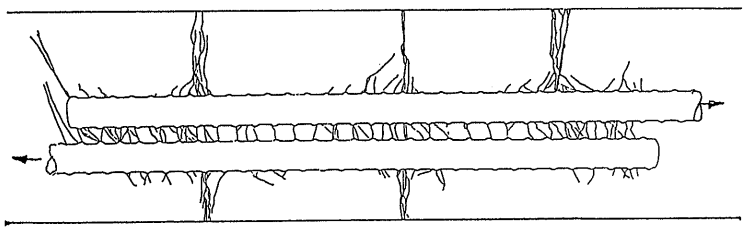

d. Reinforcing stress: 2,330 kgf/cm^2 (228 MPa)

Fig. 5 Crack growth in lapped splice specimen [5] (traced from x-ray shadowgraph film, reinforcing bar: D16; maximum size of aggregate: 5 mm)

4.3 Beam Specimen

Photograph 5 shows the fine cracks detected by radiography in the case of beam specimens (each with a cross section of 70 x 150 mm, a span of 500 mm, and one D6 reinforcing bar). In this case, in order to determine the location of cracking, a 50 mm notch was cut in the middle of the span on the tension side. The notched portion was blackened in the image by filling it with lead beforehand to prevent halation. Further, since this beam specimen had a single D6 reinforcing bar on the tension side, it was possible to prevent sudden failure of the beam, permitting the film mode to be used to observe crack growth.

Photograph 5a was taken when the load was 565 kgf (5.54 kN) and the crack opening displacement (crack width at notch entrance) 0.4 mm; it shows conditions immediately after the occurrence of minute cracks at the end of the notch. The maximum width of the cracked zone in the horizontal direction at this time was approximately 6 mm, and the maximum length 25 mm. The drawing to the right of the photograph is a tracing of the cracks taken directly from the film.

Photograph 5b was taken when the load reached 680 kgf (6.66 kN) and the crack opening displacement was 1.3 mm; the maximum width of the cracked zone in the horizontal direction at this time was approximately 9 mm and the length 56 mm. It can be seen that the number and length of the fine cracks was grown substantially.

Photograph 5c is at a load of 1,115 kgf (11.32 kN) and the maximum width of the cracked zone in the horizontal direction at this time was approximately 14 mm and the maximum length 95 mm.

As may be comprehended from these photographs, fine cracks radiate in large numbers from the end of the notch, and occurrence is within a zone of a certain width. With increasing load, the width and length of the zone gradually increases.

Figure 6 shows the load-opening displacement relationship measured at the same time as the shadowgraphs of the beam specimen was taken. The times at which the shadowgraphs of Photo. 5 were taken are shown. The temporary displacements seen in the curve are disturbances caused by pauses in loading for x-ray filming.

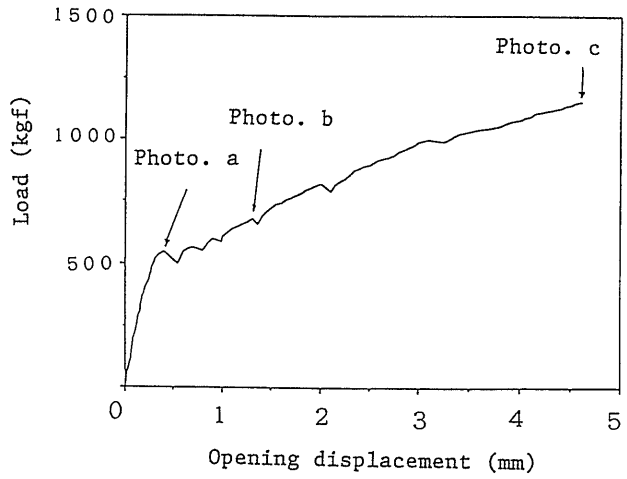

Fig. 6 Load-crack opening displacement curve of beam specimen

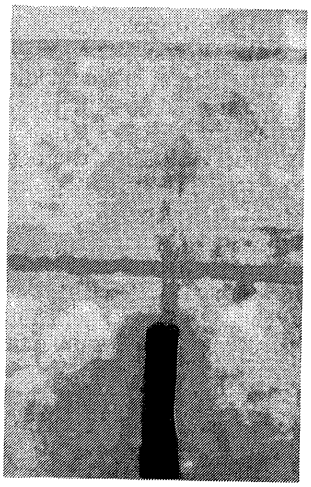

a. Load: 565 kgf (5.54 kN);
crack opening displacement: 0.4 mm

b. Load: 680 kgf (6.66 kN)
crack opening displacement: 1.3 mm

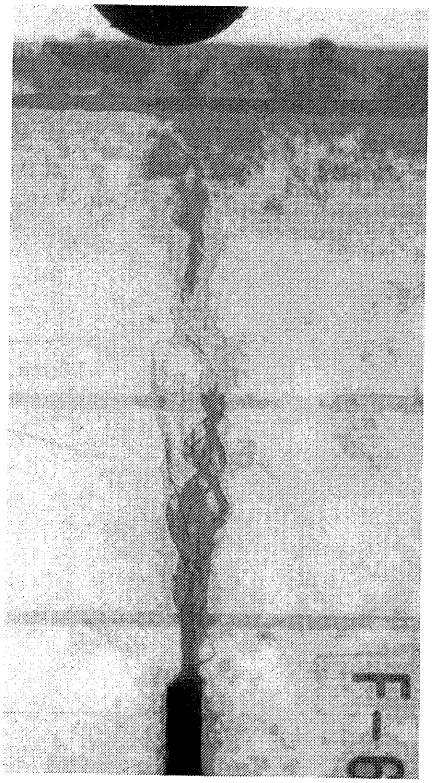

c. Load: 1,155 kgf (11.32 kN) crack opening displacement: 4.6 mm

Photo. 5 Results of fine crack detection by the x-ray technique: beam specimen (maximum size of aggregate: 15 mm; tracing from x-ray film shown at right of photograph: scale 80 %

4.4 Three-dimensional Configuration of Fine Cracks

As described in the preceding section, a comparison of the fine cracks detected by radiography and by the red ink injection method indicates that there is a difference with regard to the number of cracks formed in the vicinity of each lug on a reinforcing bar. In examining this problem, it was thought necessary to first look into whether the observation was basically of a single crack in the x-ray picture, aggregated such that it appears as multiple cracks, or whether there were actually multiple cracks from the beginning. For this purpose, it is necessary to investigate the three-dimensional configuration of the fine cracks.

Irradiating the area around comparatively large embedded objects such as reinforcing bars and defects from two directions, and thus determining their three-dimensional shape and location by analyzing the two films, are a procedure already in practical use. However, it was found through studies from various angles that with this type of method, even if contrast media were used, it was difficult to resolve the three-dimensional configuration of the fine and intricately intertwined cracks considered in this study. In the field of medicine, cross sections of the human body are now being taken by CT scanning. Further, CT scanning has recently begun to be used in industrial fields, though apparatus capable of scanning loaded specimens as used in this study is not readily obtainable. Thus this technique is as yet unavailable.

Therefore, as an alternative, a tensile specimen for axial loading (same configuration and dimensions as that described in 4.1) was tested using a contrast medium colored by adding a small amount of red ink. After radiography, the specimen was cut into six thin slices parallel to the reinforcing bar axis, as shown in Fig. 7, and the colored cracks at the individual surfaces were observed. Further, these surfaces were again stacked to examine the three-dimensional configuration of the fine cracks.

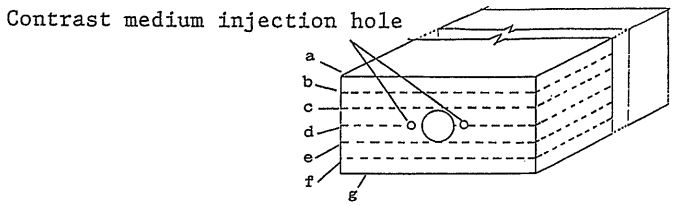

Fig. 7 Direction of slicing of specimen

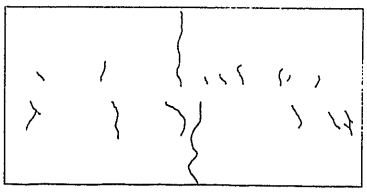

Fig. 8 Cracking in plane d

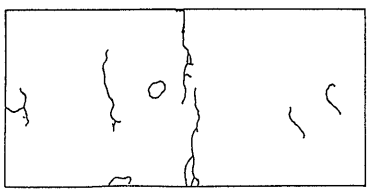

Fig. 9 Cracking in plane c

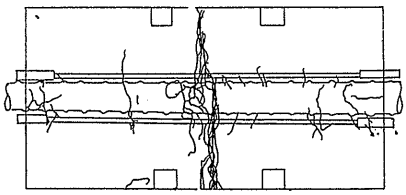

Fig. 10 Diagram of crack superpositioning at individual slice planes

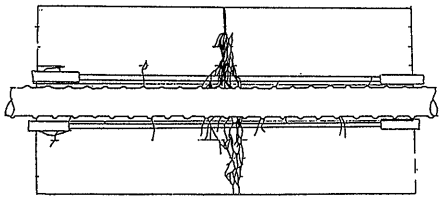

Fig. 11 Diagram traced from x-ray film of same specimen

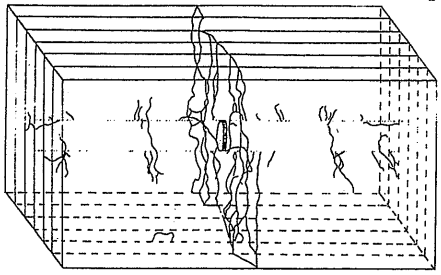

Fig. 12 Three-dimensional configurations of cracks

Figure 8 shows the cracks (colored pale red) observed on the slice taken at the plane (Plane d) including the center line. As for Fig. 9, it shows the cracking at Plane c slightly distant from the reinforcing bar surface. As these figures show, cracking at single slice is not singular, but multiple. The cracks appear to avid or wind around pieces of aggregate. However, the number of cracks is not very large. This is thought to have been because the fine cracks closed up on removing the load, squeezing out some of the red ink and making observation difficult. Further examination is required concerning this point.

Figure 10 shows the cracks observed at the slice planes with the slices again stacked together to form a composite figure. A comparison of this with Fig. 11 traced from x-ray film taken during loading of the same specimen shows that the two are similar in outline, but the zone of complex lateral cracking in the middle is slightly broader as measured by the x-ray contrast medium technique. Furthermore, on the x-ray film, there is a shadow in the form of a cloud that cannot be definitely discerned as cracking surrounding the zone of fine cracks. It may be considered a zone of even finer cracks, but this cannot be confirmed. This possible zone of fine cracks in the x-ray pictures cannot be seen at all on the cut plane of the concrete after load removal.

Figure 12 shows the cracks observed at the slice surfaces each shifted 5 mm to the right and down to display the three-dimensional configuration of the cracks. This figure also hints that the cracks are not in a simple plane, but comprise fairly complex irregularities in a layered configuration.

4.5 Influence of Aggregate Size on Fine Cracking

As mentioned in 4.4, cracks tend to meander during their growth process due to the presence of

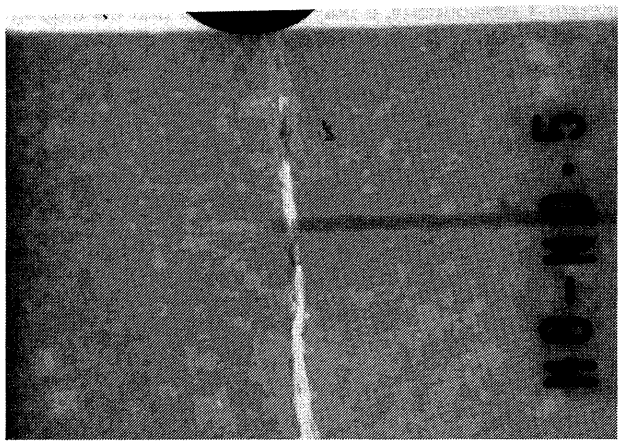

a. Maximum size of aggregate: 5 mm, maximum horizontal width of fine crack zone: 4 mm

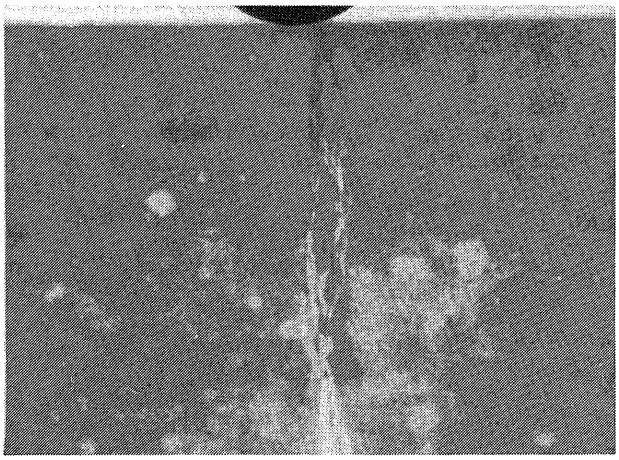

b. Maximum size of aggregate: 10 mm, maximum horizontal width of fine crack zone: 8 mm

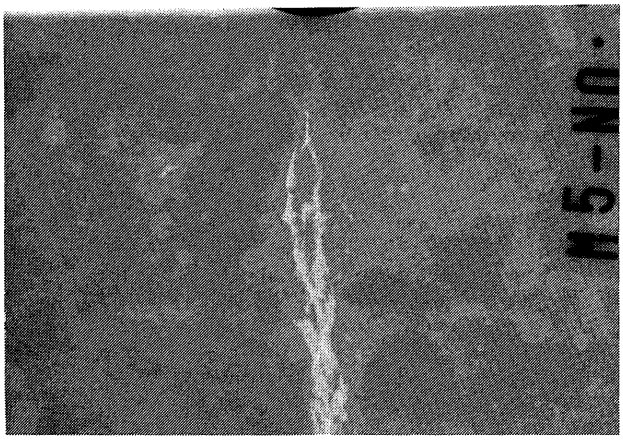

c. Maximum size of aggregate: 15 mm, maximum horizontal width of fine crack zone: 13 mm

Photo. 6 Results of detecting fine cracks by x-ray technique used to examine influence of aggregate size: beam specimen (150 x 50 x 540 mm)

aggregate in the concrete. Consequently, it may be assumed that the aggregate size affects the fine crack configuration. Experiments were conducted to investigate the effects of aggregate size. Examples of the results are given for the cases of the beam specimens in Photo 6 (a: maximum size of aggregate Gmax = 5 mm; b: Gmax = 10 mm; and c: Gmax = 15 mm). These pictures are x-ray shadowgraphs taken when cracks from notches cut at the span centers on the tension sides of beams had grown almost as far as the loading point in single-point loading. As may be seen in these photographs, the width of the zone of occurrence differs according to the maximum size of aggregate that has been used. The maximum widths of the crack zones in these cases were 4 mm for Gmax of 5 mm, 8 mm for Gmax of 10 mm, and 13 mm for Gmax of 15 mm. An examination of the results of other experiments indicates that, although there is considerable scatter in values, the tendency is for the width of the fine crack zone to be greater when the maximum aggregate size is large.

5. CONCLUSIONS

The aim of this study was to develop a technique for detecting fine cracks occurring around reinforcing bars in concrete by applying the radiography techniques generally used in the field of medicine. After investigating the properties of fine cracks around reinforcing bars in axially loaded tensile specimens, lapped splice specimens, and beam specimens using the new technique, the following conclusions can be drawn:

(1) The x-ray inspection technique developed in this study is an effective mean of nondestructively detecting fine cracks in the interior of reinforced concrete on a continuous basis. However, if this technique is to be applied to actual structures in the field, further study will be required as regards the type of contrast medium to be used and the method of injecting the medium into the concrete.

(2) In this study, a commercial iodine-based medium of iodine content 440 mg/l - as used in the medicine - was found to be most suitable.

(3) In experiments using axially loaded tensile specimens, successful detection of numerous fine cracks radiating from the lugs of the deformed bars was possible. The cracks formed a complex, intertwined network as reinforcing bar stress intensity was increased. These fine cracks, when compared with those observed by the red ink injection method, appear similar as far as overall orientation is concerned, but the number occurring from a single lug is greater, and the form is more complex.

(4) In experiments using lapped splice specimens, cracks crossed from one bar diagonally to the other at points sandwiched by the two reinforcing bars at splices, and of the number of cracks increased as the reinforcing bar stress was increased; ultimately, cracks formed along roughly the entire splice length. These fine cracks, when compared with those observed by the red ink injection method, were more or less the same in orientation, but there were far more of them.

(5) In experiments using beam specimens, fine cracks emanating from the tips of notches cut in the tension side at the span center were successfully detected, as was the condition immediately after cracking begun, the increasing number of cracks as reinforcing bar stress intensity increased, and the way in which the crack zone expanded in a complicated manner.

(6) As a result of investigating the influence of maximum aggregate size on the width of the fine crack zone, it was found that the zone increased in width with larger aggregate. This is thought to be because the fine cracks have a tendency to meander around the pieces of aggregate.

(7) Tensile specimens injected with a colored contrast medium were axially loaded and radiography performed; the specimens were then cut using a diamond saw into a number of

slices, and the condition of cracking was observed at the individual slice surfaces. It was found that cracks on individual slice surfaces were not single cracks, that near pieces of aggregate there were some cracks that branched out and wound around the aggregate, and that the cracks in general meandered. By restacking the slices, it was possible to create an image of the complex three-dimensional configuration of the fine cracks.

6. CLOSING REMARKS

The contrast media used in this study were all commercially available products used in the medical field. In order to prevent side effects on the human body, these products are mixed with various other chemicals intermixed, while same chemicals that give effective contrast are restricted as to variety and concentration. Thus the contrast medium selected for use in this study cannot be declared to be the most suitable as regards contrast performance and ability to enter cracks. Accordingly, if it were possible to develop a high-performance industrial contrast medium specifically for the usage described in this study, it is thought that the crack detection performance of this technique would be improved. As such, this study is still at a basic stage, and further progress with research will enable this new nondestructive testing method for concrete to be brought into practical use.

The research described here was proposed and planned by the author during his time at Prof. Gert Koning's laboratory at Technische Hochschule Darmstadt in the then West Germany, where he studied for a year from August 1984. The first radiographic experiment was begun on a small pull-out specimen at the laboratory of Prof. Theo Tschudi in the Physics Department of the Hochschule with his kind agreement and with the cooperation of Dr.Otto Kroggel. Lead sulfate was used as the contrast medium at that time, but no cracks within the concrete could be detected at all.

On returning to Japan, the author put together a test apparatus and began experiment in 1986. This paper is a summarization of the results obtained from the time of resumption of experiments through 1990 [3]-[7]. The author is profoundly grateful to Prof. Gert Konig, Prof. Theo Tschudi, and Dr. Otto Kroggel for their kind assistance at the time this research was initiated. The work is founded on the research of Dr. Yukimasa Goto (then a Professor at Tohoku University, presently a Professor at Tohoku Gakuin University) who discovered internal cracking around reinforcing bars by the red ink injection method. The author wishes to express his gratitude to Dr. Goto for his guidance over a period of many years. Further, the author sincerely thanks the many graduate students who have dedicated time to experiments in the course of this research work.

REFERENCES

[1] Goto, Y: Cracks formed in concrete around deformed tension bars, Journal of American Concrete Institute, Vol. 68, pp. 244-251, April 1971
[2] Goto, Y. and Otsuka, K: Cracks formed in concrete around deformed bars subjected to tension, Transactions of the Japan Society of Civil Engineers, No. 294, pp. 85-100, 1980
[3] Otsuka, K. , Morohashi, K., and Naruse, Y: Detecting cracks in concrete by radiography, Summaries of Papers, Annual Meeting, Tohoku Chapter, JSCE, Div. 5, 1987
[4] Abe, T., Otsuka, K., and Abe, Y: Detection of fine cracks in concrete by radiography, Summaries of Papers, Annual Meeting, Tohoku Chapter, JSCE, Div. 5, 1988
[5] Otsuka, K: Detection of fine cracks by x-ray technique, Proceedings of the Japan Concrete Institute, Vol. 10-3, pp. 145-150, 1988
[6] Otsuka, K: X-ray technique with contrast medium to detect fine cracks in reinforced concrete, Fracture Toughness and Fracture Energy, Balkema, Rotterdam, 1989
[7] Otsuka, K. and Shoji, Y: Detection of fracture process zone of concrete by x-ray technique, JCI Colloquium on Fracture Mechanics, Vol. II, pp. 1-4, 1990